ELSEVIER

Thermochimica Acta 272 (1996) 75–85

thermochimica acta

Sinusoidal temperature treatments in thermal analysis[1]

Dun Chen, David Dollimore*

Department of Chemistry and College of Pharmacy, University of Toledo, Toledo, OH 43606, USA

Received 27 September 1994; accepted 3 June 1995

Abstract

The use of sinusoidal temperature treatments in various thermal analysis techniques is briefly outlined. A generalized approach is described to cover all the techniques in which this approach is utilized. Using a computer simulation, the effect of a sinusoidal temperature variation on the thermogravimetric (TG) trace is investigated. This indicates under what conditions a modulated differential scanning calorimeter (DSC) temperature program can be operated when using a simultaneous DSC-TG unit. Other aspects of the computer simulation are noted.

Keywords: TG; DSC; Sinusoidal temperature

1. Introduction

Normally in thermal analysis a steadily rising temperature is imposed on a system. Often particularly with regard to phase transitions, it is recommended that a cooling curve also be examined. This identifies a kinetically reversible process from an irreversible transition. A reversible transition from a solid to a liquid will be endothermic in the rising temperature mode and exothermic on the cooling cycle. Schematically this is represented as:

$$\text{Solid A} \rightarrow \text{liquid A (endothermic)} \quad (1)$$

$$\text{Liquid A} \rightarrow \text{solid A (exothermic)} \quad (2)$$

* Corresponding author.

[1] Presented at the 23rd North American Thermal Analysis Society Conference, Toronto, Ont., Canada, 25–28 September, 1994.

SSDI 0040-6031 (95) 02603-7

The same would be true for a readily reversible solid–solid transition, e.g.

Solid A1 → solid A2 (endothermic) (3)

Solid A2 → solid A1 (exothermic) (4)

The regeneration of the original phase on cooling may not occur at the same temperature due to supercooling effects. Metastable to stable transitions are irreversible; an extreme example would be the production of a glassy state on cooling. A straightforward heating and cooling curve represents the extreme limit of modulated temperature control. Each part of a simple curve of the above kind should be reversible so, if the frequency of the temperature modulation was reduced so that the temperature entered into a cooling mode over various segments of the entire curve, the generation of a portion of the curve on the heating mode segment would be canceled out on the cooling segment. We call this a reversible signal. It is tempting to identify such a signal and dignify it with the term thermodynamic reversible but an otherwise thermodynamic signal can be rendered experimentally irreversible because of loss of material from the system. This would occur if the transition was

Liquid → vapor, i.e. boiling (5)

or

Solid → vapor, i.e. sublimation (6)

In view of this it is probably best to describe any observable sinusoidal thermal analysis as experimentally reversible on the time scale of the modulation. The signal on modulation will only completely cancel out if the events occur at exactly the same temperature on the heating curve and the cooling curve. Schematically, if

Heating: Condensed phase I → condensed phase II at T_1 (7)

and

Cooling: Condensed phase II → condensed phase I at T_2 (8)

where $T_1 \neq T_2$, i.e. the temperature on the cooling shows a transition at a different temperature to the same transition (in the opposite direction) on the heating curve then the modulated signal will not completely cancel.

In these cases the use of modulated or dynamic DSC with a sufficiently high frequency of temperature modulation overcomes some of the mismatches noted in Eqs (7) and (8). The question remains, however, does it in such instances relate to real behavior patterns or to a pattern of behavior that only occurs due to the experimental parameters imposed on it by the technique.

An amorphous or glassy material is thermodynamically unstable and may undergo an exothermic change on heating which is irreversible on cooling. Schematically,

Amorphous phase → thermodynamically stable phase (exothermic)

In a modulated temperature regime, this change will be missing on the cooling segments. The glass transition is a second order change with an abrupt change in heat capacity. It has been shown by Reading [1] how modulated DSC provides a direct method of estimating heat capacity. The exothermic and endothermic subsidiary peaks which often accompany experimentally determined T_g points using DSC can be shown to be a reversible or an irreversible component of the DSC trace using modulated DSC.

However in recent investigations of phase transitions using simultaneous DTA/TG, it was observed that a thermodynamically reversible solid to liquid transition was accompanied by significant loss in weight due to evaporation. This would have occurred if the equilibrium vapor pressure was so high that the loss in weight due to evaporation around the transition was possible. Schematically this can be represented as

Solid phase A → liquid phase + vapor phase

On cooling the above change is reversible but the mass involved is different giving less exothermic change than expected. This would mean that the modulated DSC signal would show an experimentally reversible and irreversible component.

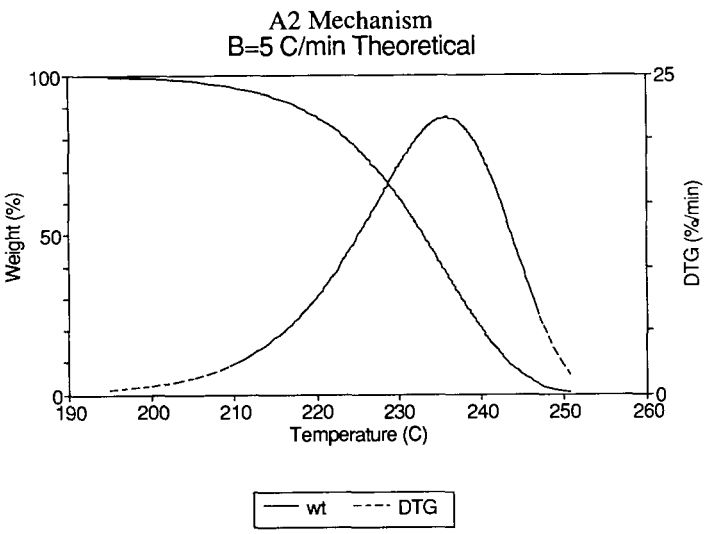

Fig. 1. Theoretical TG and DTG curves for A2 mechanism. In the figures, B is the heating rate, A is the modulation amplitude and F is the modulation cycle (or ω^{-1}, s).

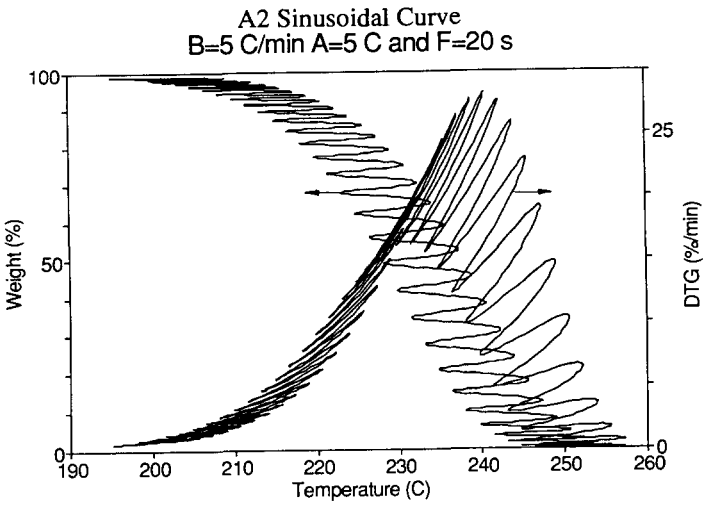

Fig. 2. TG and DTG curves for the original set data.

It was decided to find what frequency of modulation in temperature programming was necessary to produce a TG curve that did not significantly differ from the unmodulated TG curve. It was possible to show this using a computer simulation based on programming that that had been derived in a previous publication [2]. Operated within these parameters then a modulated DSC-TG unit would be possible.

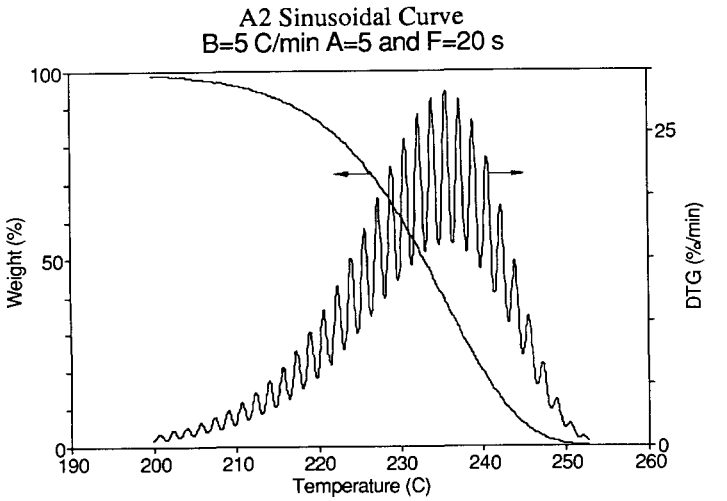

Fig. 3. TG and DTG curves for the linear set data.

2. Computer programming

In the controlled constant heating rate experiments, the programmed temperature can be expressed as

$$T = T_0 + \beta t \tag{9}$$

where T (°C) is the programmed temperature, T_0 (°C) is the initial temperature, t is the time (min) and β is the heating rate (°C min^{-1}). While in the modulated DSC experiments, the heating rate is expressed as

$$T = T_0 + \beta t + B \sin(\omega t) \tag{10}$$

where B is the amplitude of the modulation (°C) and ω is the frequency (min^{-1} or s^{-1}).

Eq. (10) is used in the data simulation program which is as discussed in previous reports [2]. The values of B and ω used were: 5, 3 and 1°C for B and 0.01, 0.05 and 0.1 s^{-1} for ω. Heating rates were 1, 3, 5 and 10°C min^{-1}. Under each condition, three sets of data were created: the "original" set which contains the original data, the "middle-point" set which only collects the values for the reaction at the $\sin(\omega t) = 0$ conditions and the "linear" simulated set which means the temperature recorded was created by using the Eq. (9) for the corresponding time in the original data set without changing other signal values.

All data were treated by computer programs to obtain the kinetic parameters. These programs were discussed in previous paper [2]. The model reaction mechanism used here is the A2 (refer to Table 1 for the meaning of the symbol in Ref. [2]). The activation energy E, is 120.00 kJ mol^{-1} and the frequency factor, A, is 1×10^{10} s^{-1}.

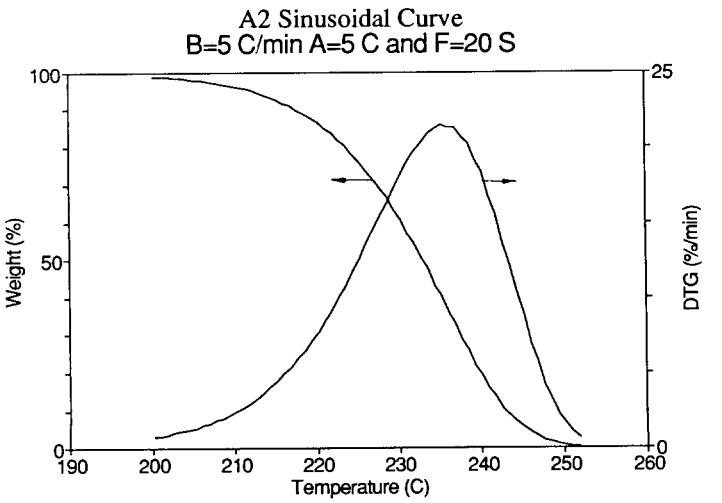

Fig. 4. TG and DTG curves for the middle-points set data.

Table 1a

Results of the kinetic evaluation using SHRD and SHRI methods for original data

B/°C	ω^{-1}/s	β/(°C min^{-1})	SHRD			SHRI		
			E/(kJ mol^{-1})	A/s^{-1}	R	E/kJ mol^{-1})	A/s^{-1}	R
5	100	10	120.03	1.01×10^{10}	1.000	118.62	7.30×10^{9}	0.9672
		5	120.01	1.00×10^{10}	1.000	111.61	1.27×10^{9}	0.9671
		2	167.22	2.44×10^{15}	0.9352	118.15	8.73×10^{9}	0.9204
		1	nf	nf	nf	nf	nf	nf
	20	10	120.02	1.01×10^{10}	1.000	112.88	1.81×10^{9}	0.9682
		5	120.01	1.00×10^{10}	1.000	112.12	1.44×10^{9}	0.9661
		2	165.48	1.56×10^{15}	0.9480	115.30	4.06×10^{9}	0.9277
		1	nf	nf	nf	nf	nf	nf
	10	10	120.02	1.01×10^{10}	1.000	113.27	1.93×10^{9}	0.9684
		5	120.01	1.00×10^{10}	1.000	111.78	1.34×10^{9}	0.9664
		2	165.32	1.50×10^{15}	0.9471	115.32	4.05×10^{9}	0.9272
		1	nf	nf	nf	nf	nf	nf
3	100	10	120.03	1.01×10^{10}	1.000	121.04	1.30×10^{10}	0.9884
		5	120.01	1.00×10^{10}	1.000	117.12	4.92×10^{9}	0.9877
		2	170.10	4.99×10^{15}	0.9437	127.83	1.07×10^{10}	0.9677
		1	249.54	2.70×10^{25}	0.9101	130.19	5.55×10^{11}	0.9046
	20	10	120.02	1.01×10^{10}	1.000	117.38	5.33×10^{9}	0.9881
		5	120.01	1.00×10^{10}	1.000	117.08	4.92×10^{9}	0.9874
		2	169.18	3.95×10^{15}	0.9456	125.97	6.63×10^{10}	0.9693
		1	nf	nf	nf	nf	nf	nf
	10	10	120.02	1.01×10^{10}	1.000	117.54	5.49×10^{9}	0.9883
		5	120.01	1.00×10^{10}	1.000	117.12	4.96×10^{9}	0.9874
		2	169.08	3.86×10^{15}	0.9464	125.80	6.28×10^{10}	0.9696
		1	nf	nf	nf	nf	nf	nf
1	100	10	120.03	1.01×10^{10}	1.000	120.96	1.26×10^{10}	0.9988
		5	120.01	1.00×10^{10}	1.000	1 19.73	9.37×10^{9}	0.9986
		2	171.56	7.17×10^{15}	0.9472	132.47	3.50×10^{11}	0.9928
		1	272.73	1.16×10^{28}	0.9170	155.30	4.62×10^{14}	0.9782
	20	10	120.02	1.01×10^{10}	1.000	119.68	9.26×10^{9}	0.9987
		5	120.01	1.00×10^{10}	1.000	119.64	9.20×10^{9}	0.9986
		2	171.05	6.30×10^{15}	0.9486	131.65	2.83×10^{11}	0.9932
		1	274.68	1.94×10^{28}	0.9134	157.07	7.39×10^{14}	0.9768
	10	10	120.02	1.01×10^{10}	1.000	119.72	9.34×10^{9}	0.9987
		5	120.01	1.00×10^{10}	1.000	119.71	9.31×10^{9}	0.9986
		2	171.03	6.26×10^{15}	0.9492	131.75	2.88×10^{11}	0.9934
		1	274.40	1.81×10^{28}	0.9107	157.09	7.49×10^{14}	0.9757

Note: In the table, B is the modulation amplitude and ω is the modulation frequency. β is the heating rate, E is the activation energy, A is the frequency and R is the regression factor. nf means the R value is lower than 0.9000 and no kinetic evaluation was performed.

Table 1b

Kinetic evaluation results from MHRD and MHRI methods for original data

B/°C	ω^{-1}/s	MHRD		MHRI	
		E/(kJ mol^{-1})	σd/(kJ mol^{-1})	E/(kJ mol^{-1})	σd/(kJ mol^{-1})
5	100	52.48	21.75	77.39	9.74
	20	52.88	20.94	77.36	6.48
	10	55.88	18.93	74.41	7.95
3	100	52.77	21.75	77.00	9.58
	20	52.59	20.97	76.96	6.80
	10	54.19	21.32	75.93	6.83
1	100	53.11	21.57	76.99	9.66
	20	53.14	20.95	77.37	6.47
	10	53.38	21.08	76.89	4.46

Note: σd in the table means the standard deviation. For the meanings of other symbols, please refer to the note in Table 1a.

Graphs were created by using the Quattro Pro software on an IBM personal computer.

3. Results and discussion

Fig. 1 shows the TG and DTG curves for the theoretical A2 mechanism at a heating rate of 5°C min^{-1} without any temperature modulation. When the temperature modulation was introduced, 5°C at a period of 20 s, the figures for the three sets of data are shown in Figs. 2–4. It can be seen that the reactions occur over the same temperature range although the DTG signals vary one from another. However, TG and DTG curves for the middle-point set data (Fig. 4) show a very good agreement to the theoretical figure (Fig. 1).

The kinetic evaluation results from SHRD, SHRI, MHRD and MHRI methods are listed in Tables 1–3. From the results in Tables 1a and 2a, it can be seen that, when the heating rate is slower than 2°C min^{-1}, the calculated activation energy values from SHRD and SHRI methods show a large deviation from the theoretical value with relatively low R values. These results suggest that the use of the original and linear sets of data can provide good kinetic evaluation information when a relatively high heating rate is used, in this study, faster than 5°C min^{-1}. However, when the results in Table 3a are considered, there is no difference whatever with the heating rate used. This is due to the sinusoidal signals used in the original and the linear sets of data.

By comparing the E, A and R values in Tables 1a, 2a and 3a, it can be seen that the middle-point set data provides the best result. This is due to the sinusoidal $d\alpha/dt$ signal used in the original and linear sets of data. At the same time, the TG curve is affected by the sinusoidal temperature programming which is shown as the small fluctuation on the TG curve in Fig. 3. Both reasons cause the incorrect E, A and R values. When the E and

Table 2a

Kinetic evaluation results from SHRD and SHRI methods for linear data

B/ °C	ω^{-1}/s	β/(°C min^{-1})	SHRD			SHRI		
			E/(kJ mol^{-1})	A/s^{-1}	R	E/kJ mol^{-1})	A/s^{-1}	R
5	100	10	113.10	2.24×10^{9}	0.9710	119.08	8.21×10^{9}	0.9993
		5	121.03	1.29×10^{10}	0.9709	119.90	1.01×10^{10}	0.9998
		2	171.26	6.77×10^{15}	0.9216	132.61	3.73×10^{11}	0.9959
		1	nf	nf	nf	159.48	1.48×10^{15}	0.9886
	20	10	119.72	9.39×10^{9}	0.9721	119.60	9.40×10^{9}	0.9999
		5	120.38	1.09×10^{10}	0.9705	119.59	9.37×10^{9}	1.000
		2	171.08	6.43×10^{15}	0.9199	131.96	3.15×10^{11}	0.9964
		1	nf	nf	nf	160.07	1.74×10^{15}	0.9879
	10	10	119.41	8.68×10^{9}	0.9723	119.62	9.11×10^{9}	1.000
		5	120.38	1.09×10^{10}	0.9705	119.59	9.42×10^{9}	1.000
		2	171.44	7.27×10^{15}	0.9210	132.13	3.29×10^{11}	0.9962
		1	nf	nf	nf	160.05	1.72×10^{15}	0.9879
3	100	10	116.20	4.08×10^{9}	0.9897	119.50	8.94×10^{9}	0.9997
		5	120.09	1.02×10^{10}	0.9891	120.01	1.02×10^{10}	0.9999
		2	170.84	6.01×10^{15}	0.9395	132.62	3.66×10^{11}	0.9961
		1	277.11	3.70×10^{28}	0.9016	159.69	1.52×10^{15}	0.9884
	20	10	119.97	9.96×10^{9}	0.9898	119.81	9.68×10^{9}	1.000
		5	119.95	9.89×10^{9}	0.9889	119.82	9.78×10^{9}	1.000
		2	171.79	7.62×10^{15}	0.9383	132.47	3.52×10^{11}	0.9962
		1	278.31	5.09×10^{28}	0.9018	160.49	1.89×10^{15}	0.9878
	10	10	119.67	9.23×10^{9}	0.9898	119.83	9.61×10^{9}	1.000
		5	119.83	9.59×10^{9}	0.9890	119.83	9.75×10^{9}	1.000
		2	171.76	7.56×10^{15}	0.9383	132.44	3.40×10^{11}	0.9962
		1	277.82	4.48×10^{28}	0.9012	160.42	1.85×10^{15}	0.9879
1	100	10	118.73	7.42×10^{9}	0.9989	119.85	9.64×10^{9}	1.000
		5	119.97	9.93×10^{9}	0.9988	120.01	1.00×10^{10}	1.000
		2	171.25	6.62×10^{15}	0.9476	132.59	3.60×10^{11}	0.9962
		1	277.66	4.24×10^{28}	0.9133	160.40	1.82×10^{15}	0.9879
	20	10	120.02	1.01×10^{10}	0.9988	119.94	9.86×10^{9}	1.000
		5	119.99	9.99×10^{9}	0.9988	119.94	9.91×10^{9}	1.000
		2	171.44	6.94×10^{15}	0.9476	132.51	3.52×10^{11}	0.9963
		1	277.68	4.26×10^{28}	0.9129	160.51	1.87×10^{15}	0.9878
	10	10	119.95	9.88×10^{9}	0.9989	119.94	9.86×10^{9}	1.000
		5	119.94	9.84×10^{9}	0.9988	119.94	9.87×10^{9}	1.000
		2	171.22	6.57×10^{15}	0.9477	132.49	3.51×10^{11}	0.9963
		1	278.09	4.75×10^{28}	0.9130	160.74	1.99×10^{15}	0.9877

Note: Please refer to the note in Table 1a for the meaning of symbols.

R values from the SHRD and SHRI methods in Table 2a are compared, it is shown that the SHRI method will provide better values of E, A and R. This is because the oscillating $d\alpha/dt$ value from the DTG curve is not used in the kinetic calculation using the SHRI

Table 2b

Kinetic evaluation results from MHRD and MHRI methods for linear data

B/°C	ω^{-1}/s	MHRD		MHRI	
		E/(kJ mol^{-1})	σd/(kJ mol^{-1})	E/(kJ mol^{-1})	σd/(kJ mol^{-1})
5	100	52.81	22.64	77.15	5.64
	20	51.86	22.73	77.37	4.35
	10	55.76	20.77	76.54	5.02
3	100	52.65	22.12	77.10	4.35
	20	52.22	22.80	77.29	4.25
	10	55.27	22.65	76.95	4.52
1	100	53.29	22.56	77.08	3.26
	20	53.27	22.63	77.12	3.88
	10	53.54	22.80	77.03	3.07

Note: Please refer to the note in Table 1b for the meaning of symbols.

method. The oscillating temperature program imposed on the TG curve (Fig. 3) is responsible for the non-agreement values of E and A from the SHRI method.

When multiple heating rate methods are considered, it can be seen from Tables 1b, 2b and 3b, that the MHRI method will provide better values of E and a smaller standard deviation. This is because the oscillating $d\alpha/dt$ value from the DTG curve is not used in the MHRI method. However, the middle-point set data provides the E values.

From the above discussion, it can be seen that the middle-point data set provides the best calculated E, A and R values from the SHRD and SHRI methods. At the same time, the best values of E can be obtained from the multi-heating rate methods. This is due to the elimination of the sinusoidal effect on the TG and DTG signals. However, the limitation of the total data points collected in the reaction temperature range is very important and will affect the calculated result. This suggests the use of high frequency in operating the sinusoidal modulations in a simultaneous DSC-TG unit.

4. Conclusions

A theoretical study of sinusoidal temperature programming is performed. The results show that the data collected at the middle-point provided the best kinetic evaluation. This means the combination of the modulated DSC and TGA is theoretically possible and will still allow kinetic aspects of the sample to be considered in a meaningful manner.

However, the accuracy of obtaining such middle-point data is related to the sample's heat capacity and mechanical properties. If a high frequency of modulation is used then this will require good temperature measurement and control. The normal temperature fluctuation shown in most so-called linear heating rate experiments is actually the extreme condition of the sinusoidal temperature programming but the modulation in such cases is not controlled.

Table 3a
Kinetic evaluation results from SHRD and SHRI methods for middle-point data

B/ °C	ω^{-1}/s	β/(°C min^{-1})	SHRD			SHRI		
			E/(kJ mol^{-1})	A/s^{-1}	R	E/kJ mol^{-1})	A/s^{-1}	R
5	100	10	120.02	1.00×10^{10}	1.000	119.16	8.43×10^{9}	0.9979
		5	120.01	1.00×10^{10}	1.000	120.32	1.13×10^{0}	0.9994
		2	120.00	1.00×10^{10}	1.000	119.54	9.20×10^{9}	1.000
		1	120.00	1.00×10^{10}	1.000	119.53	9.20×10^{9}	1.000
	20	10	120.02	1.00×10^{10}	1.000	119.60	9.40×10^{9}	0.9999
		5	120.02	1.00×10^{10}	1.000	119.61	9.41×10^{9}	1.000
		2	120.01	1.00×10^{10}	1.000	119.56	9.20×10^{9}	1.000
		1	120.00	1.00×10^{10}	1.000	119.54	9.32×10^{9}	1.000
	10	10	120.02	1.00×10^{10}	1.000	119.59	9.06×10^{9}	1.000
		5	120.01	1.00×10^{10}	1.000	119.60	9.43×10^{9}	1.000
		2	120.01	1.00×1010	1.000	119.56	9.28×10^{9}	1.000
		1	120.00	1.00×10^{10}	1.000	119.54	8.93×10^{9}	1.000
3	100	10	120.01	1.00×10^{10}	1.000	119.32	8.61×10^{9}	0.9978
		5	120.01	1.00×10^{10}	1.000	119.90	9.89×10^{9}	0.9999
		2	120.01	1.00×1010	1.000	119.80	9.47×10^{9}	1.000
		1	120.00	1.00×10^{10}	1.000	119.80	9.54×10^{9}	1.000
	20	10	120.02	1.00×10^{10}	1.000	119.78	9.59×10^{9}	1.000
		5	120.01	1.00×10^{10}	1.000	119.84	9.81×10^{9}	1.000
		2	120.01	1.00×10^{10}	1.000	119.82	9.53×10^{9}	1.000
		1	20.00	1.00×10^{10}	1.000	119.81	9.67×10^{9}	1.000
	10	10	120.02	1.01×10^{10}	1.000	119.82	9.58×10^{9}	1.000
		5	120.01	1.00×10^{10}	1.000	119.82	9.75×10^{9}	1.000
		2	120.01	1.00×10^{10}	1.000	119.81	9.69×10^{9}	1.000
		1	120.00	1.00×10^{10}	1.000	119.81	9.51×10^{9}	1.000
1	100	10	120.02	1.00×10^{10}	1.000	119.80	9.57×10^{9}	1.000
		5	120.01	1.00×10^{10}	1.000	119.97	9.96×10^{9}	1.000
		2	120.00	1.00×10^{10}	1.000	119.94	9.82×10^{9}	1.000
		1	120.00	1.00×10^{10}	1.000	119.95	9.86×10^{9}	1.000
	20	10	120.02	1.00×10^{10}	1.000	119.92	9.83×10^{9}	1.000
		5	120.01	1.00×10^{10}	1.000	119.94	9.90×10^{9}	1.000
		2	120.01	1.00×10^{10}	1.000	119.94	9.89×10^{9}	1.000
		1	120.00	1.00×10^{10}	1.000	119.94	9.92×10^{9}	1.000
	10	10	120.02	1.01×10^{10}	1.000	119.94	9.86×10^{9}	1.000
		5	120.01	1.00×10^{10}	1.000	119.94	9.87×10^{9}	1.000
		2	120.01	1.00×10^{10}	1.000	119.94	9.89×10^{9}	1.000
		1	120.00	1.00×10^{10}	1.000	119.95	9.84×10^{9}	1.000

Note: Please refer to the note in Table 1a for the meaning of symbols.

Table 3b

Kinetic evaluation results from MHRD and MHRI methods for middle-point data

B/°C	ω^{-1}/s	MHRD		MHRI	
		E/(kJ mol^{-1})	σd/(kJ mol^{-1})	E/(kJ mol^{-1})	σd/(kJ mol^{-1})
5	100	112.37	14.94	121.85	7.79
	20	119.69	2.81	121.34	1.13
	10	120.03	0.74	121.79	0.63
3	100	112.71	12.56	122.95	7.07
	20	119.88	2.92	122.52	1.01
	10	120.43	0.82	121.15	0.60
1	100	115.62	10.26	120.78	6.54
	20	119.46	2.75	122.01	1.12
	10	120.09	0.52	121.59	0.65

Note: Please refer to the note in Table 1b for the meaning of symbols.

References

[1] M. Reading, D. Elliott and V.L. Hill, J. Thermal Anal., 40 (1993) 949.
[2] D. Chen, X. Gao and D. Dollimore, Anal. Instr., 20 (1992) 137.